LAWRENCE
LIVERMORE
NATIONAL
LABORATORY

LLNL-JRNL-638518

Sphingolipid Domains in the Plasma Membranes of Fibroblasts are Not Enriched with Cholesterol

J. F. Frisz, H. A. Klitzing, K. Lou, I. D. Hutcheon, P. K. Weber, J. Zimmerberg, M. L. Kraft

June 6, 2013

Journal of Biological Chemistry

Disclaimer

Sphingolipid Domains in the Plasma Membranes of Fibroblasts are Not Enriched with Cholesterol

Jessica F. Frisz[†], Haley A. Klitzing[†], Kaiyan Lou[†], Ian D. Hutcheon[§], Peter K. Weber[§], Joshua Zimmerberg[‡], Mary L. Kraft[†]

[†]School of Chemical Sciences, University of Illinois, Urbana, IL 61801

[§]Glenn T. Seaborg Institute, Lawrence Livermore National Laboratory, Livermore, CA 94551

[‡]Program in Physical Biology, Eunice Kennedy Shriver National Institute of Child Health and Human Development, National Institutes of Health, Bethesda, MD 20892

Abstract

The plasma membrane is widely expected to contain domains that are enriched with cholesterol and sphingolipids. We tested this hypothesis by directly imaging metabolically incorporated isotope-labeled cholesterol and sphingolipids within the plasma membranes of intact cells with high-resolution secondary ion mass spectrometry (SIMS). Though acute cholesterol depletion reduces sphingolipid domain abundance, cholesterol was not enriched within the sphingolipid domains, and was instead evenly distributed throughout the plasma membrane. Thus, we rule out favorable cholesterol – sphingolipid interactions as dictating plasma membrane organization. Instead, cholesterol affects sphingolipid organization via an indirect mechanism that involves the cytoskeleton and presently unidentified cellular components.

Introduction

While cholesterol concentration is known to vary between different organelles (*1*), the cholesterol distribution within the plasma membrane is the subject of debate (*2*). According to one hypothesis, the plasma membrane contains small (<200 nm in diameter) and dynamic domains that are enriched with cholesterol and sphingolipids (*3*). These domains, which are referred to as the lipid rafts, are postulated to result from cohesive interactions between cholesterol, sphingolipids, and select membrane proteins (*3*). Though the cholesterol-dependent biophysical behaviors of sphingolipids have been characterized (*4*), until recently, the distributions of cholesterol and most lipid species in the plasma membrane could not be directly imaged without using potentially perturbing labels.

A high-resolution imaging secondary ion mass spectrometry (SIMS) technique (performed on a Cameca NanoSIMS 50) that preserves biomolecule organization in membranes or cellular compartments (*5-9*) has enabled mapping the distributions of rare isotope-labeled lipids in the plasma membrane (*9-11*). Our earlier imaging of the distributions of metabolically incorporated ^{15}N-sphingolipids in the plasma membranes of mouse fibroblast cells that stably express influenza hemagglutinin (Clone 15) revealed micrometer-scale sphingolipid patches in the plasma membrane (*11*). By comparing this sphingolipid organization to those exhibited by hemagglutinin-free mouse fibroblast cells (NIH 3T3, the parent line from which Clone 15 was derived) or induced by specific drug treatments, we probed the mechanisms of plasma membrane organization (*11*). The sphingolipid domains were strongly perturbed by disruption of the cytoskeleton, moderately perturbed by a reduction in cellular cholesterol, and insensitive to hemagglutinin in the plasma membrane (*11*). These results support a model in which the cytoskeleton and its associated proteins organize the lipids within the plasma membrane.

However, the mechanism by which cellular cholesterol abundance modulates the sphingolipid organization in the plasma membrane remains unclear.

We now probe the role of cholesterol in establishing the sphingolipid domains by imaging the ^{15}N-sphingolipid distribution with respect to the ^{18}O-cholesterol within the plasma membranes of fibroblast cells. We assess whether the ^{18}O-cholesterol is enriched at the ^{15}N-sphingolipid domains, as predicted by the long-standing hypothesis that favorable cholesterol-sphingolipid interactions drive the preferential association of these two components within the plasma membrane (*3, 12*). We also characterize the effects of acute cholesterol depletion on the cholesterol and sphingolipid distribution within the plasma membrane.

We studied Clone 15 cells that had been metabolically labeled such that approximately 90% of the cellular sphingolipids contained one nitrogen-15 isotope, and approximately 60% of the cellular cholesterol contained one oxygen-18 isotope. After chemically fixing the cells with a method that does not alter lipid distribution in the membrane (*11*), cells with normal morphologies were identified by imaging with low-voltage scanning electron microscopy (SEM). The SEM image of a representative Clone 15 cell is shown in Figure 1a, where high-resolution SIMS analysis was subsequently performed at the outlined region. Plasma membrane domains with elevated ^{15}N-enrichment, and thus, high ^{15}N-sphingolipid abundance, are visible in the mosaic of ^{15}N-enrichment high-resolution SIMS images of the representative Clone 15 cell (Figure 1b). Statistical analysis indicated that ^{15}N-enrichment factors greater than 16.3 are statistically significant increases that correspond to ^{15}N-sphingolipid-enriched domains (mean (μ) ^{15}N-enrichment factor for domain-free regions = 7.5, 1 s.d. = 4.4). Surprisingly, the ^{18}O-enrichment images of the same cell do not reveal cholesterol-enriched domains. The ^{18}O-cholesterol instead appears to be evenly distributed within the plasma membrane (Figure 1c). No

difference in the ^{18}O-cholesterol abundance within the sphingolipid domain and non-domain regions was detected by visual inspection or a Kolmogorov-Smirnov statistical test ($p = 0.96$, Table 1). Similar ^{15}N-sphingolipid and ^{18}O-cholesterol distributions were observed on the four other Clone 15 cells we examined (for example, see Fig. S1), and Kolmogorov-Smirnov tests confirmed that the ^{15}N-sphingolipid domains on these cells were not enriched with ^{18}O-cholesterol ($p = 0.80$, 0.54, 0.49, and 0.60; Table 1).

We also confirmed that the hemagglutinin within the plasma membranes of the Clone 15 cells did not affect the sphingolipid and cholesterol organization by analyzing analogous mouse fibroblast cells that did not express hemagglutinin (NIH 3T3 cells). Plasma membrane domains that were enriched with ^{15}N-sphingolipids were detected on the four hemagglutinin-free NIH 3T3 mouse fibroblast cells we examined, whereas the ^{18}O-cholesterol still appeared to be evenly distributed in the plasma membrane (Figure 2 and Figure S2). A Kolmogorov-Smirnov test of the ^{18}O-enrichments in the domain and non-domain regions on the NIH 3T3 cell shown in Figure 2 revealed a small (5%) but statistically significant elevation in the ^{18}O-cholesterol abundance within the ^{15}N-sphingolipid domains ($p = 0.03$, Table 1). Based on a 0.51/1 cholesterol to phospholipid ratio (mole/mole) in the plasma membrane (*13*), this 5% elevation corresponds to a < 2 mole% increase in cholesterol in the sphingolipid domains. Substantially larger increases in cholesterol abundance are predicted by phase diagrams for vesicles composed of cholesterol, *N*-palmitoyl sphingomyelin, and the most abundant cellular phosphatidylcholine (16:0-18:1 PC) at 37 °C (*14*). No significant differences in the ^{18}O-enrichments in the domain and non-domain regions of the plasma membrane were detected on the other three NIH 3T3 cells (Kolmogorov-Smirnov test, $p = 0.17$, 0.11, and 0.73; Table 1). Based on the lack of a reproducible, statistically

significant increase in cholesterol within the sphingolipid domains, we conclude that the sphingolipid domains in the plasma membrane are not consistently enriched with cholesterol.

The lack of consistent cholesterol enrichment within the micrometer-scale sphingolipid domains suggests that cohesive cholesterol-sphingolipid interactions are not responsible for domain formation. Yet, the abundance and long-range organization of the sphingolipid microdomains in the plasma membrane are reduced by acute depletion of cellular cholesterol with methyl-β-cyclodextrin (mβCD) (*11*). To further investigate the potential role of cohesive cholesterol-sphingolipid interactions, we assessed whether mβCD treatment induced a difference in the cholesterol abundance within the sphingolipid domain and non-domain regions of the plasma membrane. Such changes in cholesterol distribution might occur if the plasma membrane's composition prior to mβCD treatment was near a critical point (*15*), or if mβCD preferentially removed cholesterol from specific membrane domains (*16*). We reduced the cholesterol abundance in metabolically labeled Clone 15 cells by approximately 30% with mβCD. Low voltage SEM imaging suggests that this level of cholesterol depletion slightly changed the cell morphology and reduced the cell spreading area (Figure 3a, Figure S3a-b), which is consistent with the known side-effects of mβCD treatment (*17*). In agreement with our earlier report (citation), the mβCD-treated Clone 15 cells had fewer ^{15}N-sphingolipid microdomains in their plasma membranes (Figure 3b, Figure S3c-d) than untreated cells, but more ^{15}N-sphingolipid domains than cells with disrupted cytoskeletons (Figure S4). The ^{18}O-enrichment images show that although mβCD treatment reduced the amount of ^{18}O-cholesterol on the cell surface, the remaining ^{18}O-cholesterol appeared to be evenly distributed in the plasma membrane (Figure 3c, Figure S3e-f). No significant difference in the ^{18}O-cholesterol abundance in the sphingolipid domain and non-domain regions was detected on the two mβCD-treated cells

we examined (shown in Figure 3c and Figure S3e, Kolmogorov-Smirnov test, p = 0.90 and 0.92, respectively, Table 1). However, Kolmogorov-Smirnov tests revealed a statistically significant increase in ^{18}O-cholesterol in the sphingolipid domains on the third mβCD-treated cell (p = 0.04, Table 1), but a statistically significant *reduction* in ^{18}O-cholesterol in the domains on the fourth mβCD-treated cell (p = 0.05, Table 1) (Figure S3f). These results demonstrate that mβCD does not preferentially remove cholesterol from sphingolipid domain or non-domain regions, or substantially alter its localization within the plasma membrane.

A combination of metabolically incorporated stable isotope labels and high-resolution SIMS has allowed us to image the cholesterol distribution with respect to sphingolipids, and compare the cholesterol abundance at discrete regions within the plasma membrane. We found that the cholesterol is not enriched within the sphingolipid domains, and is instead evenly distributed within the plasma membrane. Treatment with mβCD did not alter this even cholesterol distribution, but did reduce the abundance of sphingolipid domains within the plasma membrane. These findings provide insight into the nature of the sphingolipid domains in the plasma membrane, and the mechanisms that form them. We had previously deduced that the sphingolipid domains were not lipid rafts due to their micrometer-scale dimensions (lipid rafts are <200 nm) (*3*, *15*), and their higher sensitivity to cytoskeleton disruption than cholesterol depletion. Our finding that these sphingolipid domains are not enriched with cholesterol, which is a critical characteristic of lipid rafts (*3*), definitively confirms this deduction. Furthermore, the lack of cholesterol-enriched plasma membrane domains indicates that if lipid rafts exist, they are either smaller than our lateral resolution, or their abundance is insignificant relative to the more dominant sphingolipid-enriched domains within the plasma membrane.

The absence of cholesterol enrichment in the sphingolipid domains and the lack of location-specific cholesterol depletion following mβCD treatment demonstrate that cohesive cholesterol – sphingolipid interactions are not responsible for sphingolipid domain formation. Consequently, the reduction in sphingolipid domain abundance following mβCD treatment is not due to a loss of cohesive cholesterol-sphingolipid interactions. Instead, the effects of cholesterol depletion must be indirectly translated into changes in sphingolipid organization through the involvement of other, presently unidentified, cellular components. We anticipate that a similar mechanism in which cholesterol plays an indirect role underlies the observed cholesterol sensitivity of endocytosis, intracellular traffic, cell adhesion, and other cellular processes (*17-19*). Overall, the dependency of the sphingolipid domains on an intact cytoskeleton supports a plasma membrane model in which lipid and protein organization is actively established by remodeling of the cortical actin (*20, 21*), and cholesterol is indirectly involved in this process. By supplementing fluorescence microscopy studies with complementary high-resolution SIMS imaging of isotope-labeled lipids in the plasma membrane, the mechanism that links lipids to the cytoskeleton and the role of cholesterol in this process may be elucidated.

Acknowledgements

We thank C. Ramon and W. Hanafin for technical assistance and L. Nittler for software development. Portions of this work were carried out in the Metabolomics Center in the Roy J. Carver Biotechnology Center (University of Illinois) and the Frederick Seitz Materials Research Laboratory Central Facilities (University of Illinois), which is partially supported by U. S. Department of Energy Grant DE-FG02-07ER46471. Work at Lawrence Livermore National Laboratory performed under the auspices of the U.S. Department of Energy under Contract DE-AC52-07NA27344.

LLNL-JRNL-638518

Tables, Figures and Captions

Table 1. Statistical comparison of ^{18}O-enrichments measured in sphingolipid domain and nondomain regions within the plasma membranes of various cells.

Cell	^{18}O-enrichment, μ ± 1 s.d.		p value, Kolmogorov-Smirnov test that ^{18}O-enrichment in domains and nondomains are the same	Reject hypothesis that ^{18}O-enrichment in the domains and non-domains are the same (at 95% CI)?
	Domains	Nondomains		
Clone 15 cell 1	4.0 ± 0.8	3.9 ± 0.9	0.96	No
Clone 15 cell 2	5.7 ± 1.4	5.6 ± 1.6	0.80	No
Clone 15 cell 3	5.1 ± 2.8	5.4 ± 3.8	0.54	No
Clone 15 cell 4	4.3 ± 1.0	3.7 ± 1.3	0.49	No
Clone 15 cell 5	4.5 ± 1.0	3.7 ± 1.3	0.60	No
NIH 3T3 cell 1	5.6 ± 1.9	5.4 ± 0.8	0.03	Yes, ^{18}O-enrichment in domains > nondomains
NIH 3T3 cell 2	2.9 ± 0.3	2.6 ± 0.3	0.17	No
NIH 3T3 cell 3	3.2 ± 0.1	2.8 ± 0.3	0.11	No
NIH 3T3 cell 4	4.0 ± 1.4	3.4 ± 0.7	0.73	No
mβCD-treated Clone 15 cell 1	3.7 ± 1.3	3.9 ± 1.9	0.90	No
mβCD-treated Clone 15 cell 2	3.8 ± 2.0	3.3 ± 1.1	0.92	No
mβCD-treated Clone 15 cell 3	4.1 ± 1.9	4.2 ± 1.9	0.04	Yes, ^{18}O-enrichment in domains > nondomains
mβCD-treated Clone 15 cell 4	1.9 ± 0.8	4.7 ± 2.8	0.05	Yes, ^{18}O-enrichment in domains < nondomains

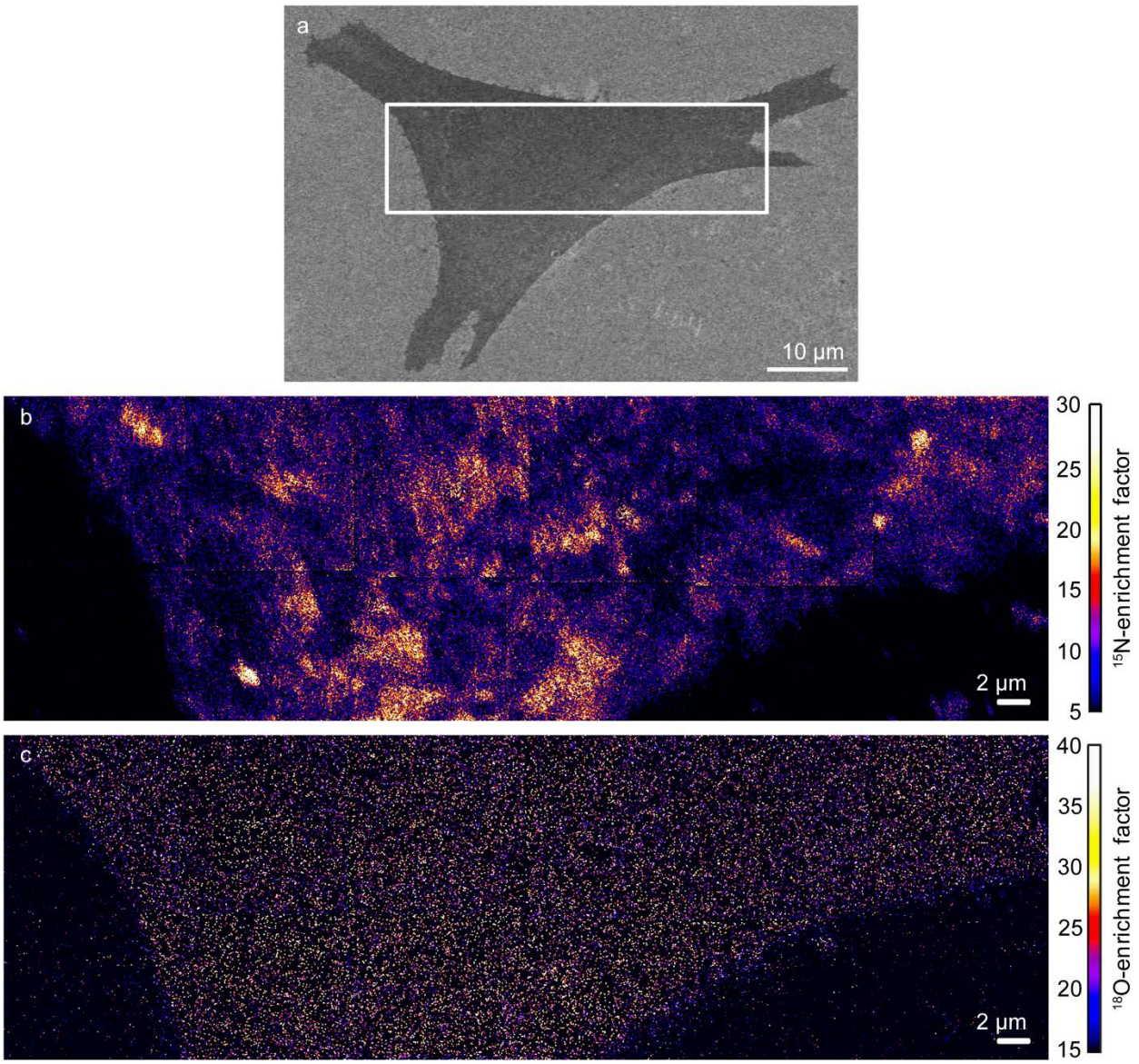

Figure 1. SEM and high-resolution SIMS images of a metabolically labeled Clone 15 fibroblast cell. (a) SEM image shows cell morphology. The outlined region shows the approximate location that was analyzed with high-resolution SIMS. (b) The mosaic of 15 × 15 µm ^{15}N-enrichment images of the cell shows the ^{15}N-sphinoglipid distribution within the plasma membrane. Domains enriched with ^{15}N-sphinoglipids (yellow and white regions) are visible in the plasma membrane. (c) The mosaic of 15 × 15 µm ^{18}O-enrichment images of the same location shows the ^{18}O-cholesterol is evenly distributed within the plasma membrane. Statistical tests confirmed the sphingolipid domains were not enriched with ^{18}O-cholesterol (Kolmogorov-Smirnov test, $p = 0.96$).

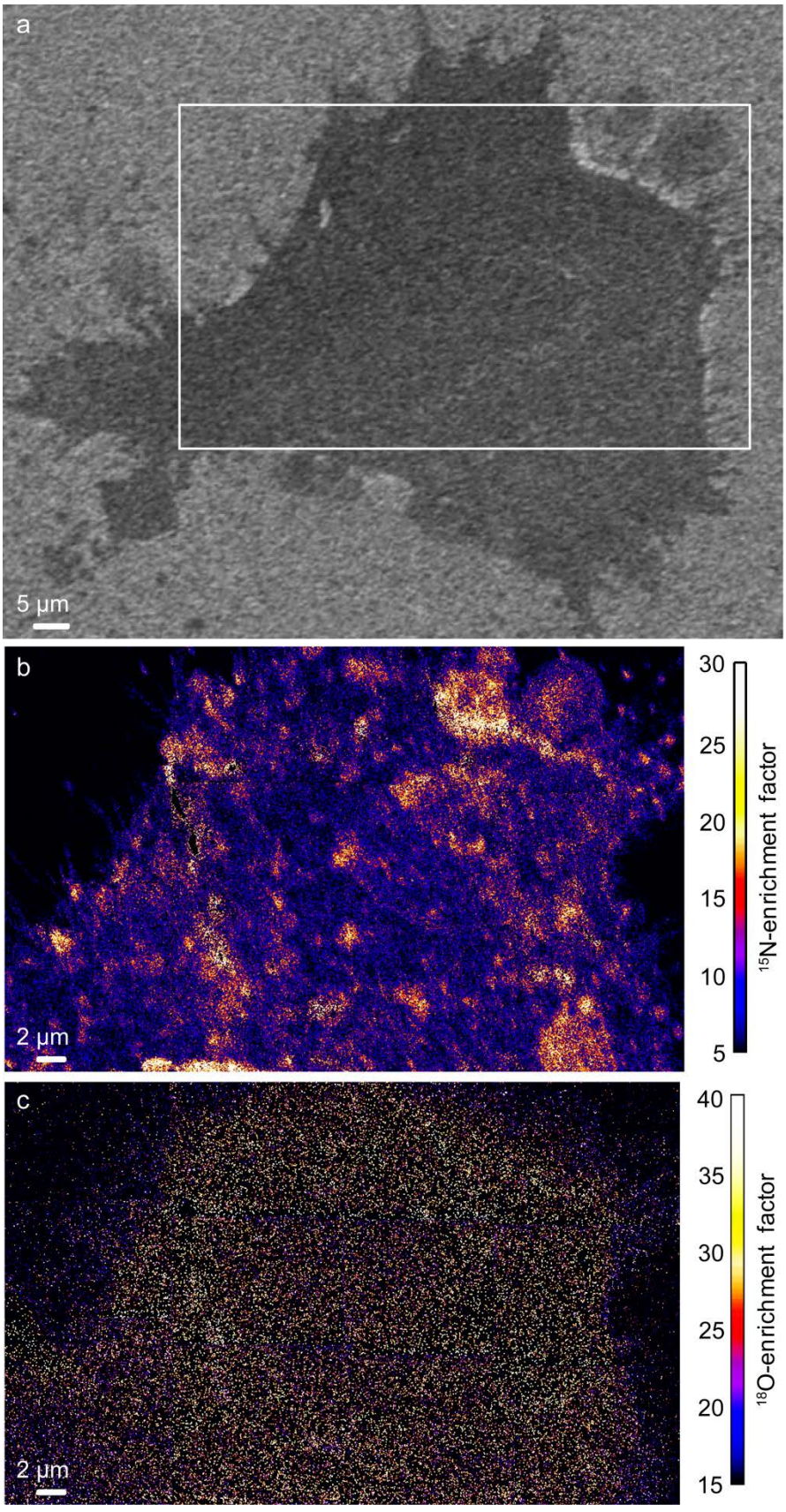

Figure 2. SEM and SIMS images of a NIH 3T3 mouse fibroblast cell that did not express the influenza membrane protein, hemagglutinin. (a) SEM image shows cell morphology. The outline marks the approximate location that was subsequently imaged with high-resolution SIMS. (b) The mosaic of 15 × 15 µm ^{15}N-enrichment images of the cell reveals domains enriched with ^{15}N-sphingolipids (yellow and white regions) in the plasma membrane. (c) The mosaic of 15 × 15 µm ^{18}O-enrichment images that werer acquired at the region outlined in (a) shows that the ^{18}O-cholesterol distribution in the plasma

membrane. The ^{15}N-sphingolipid domains on this cell, but not others (see text) contained a small (5%) but statistically significant elevation in ^{18}O-cholesterol (Kolmogorov-Smirnov test, p = 0.03).

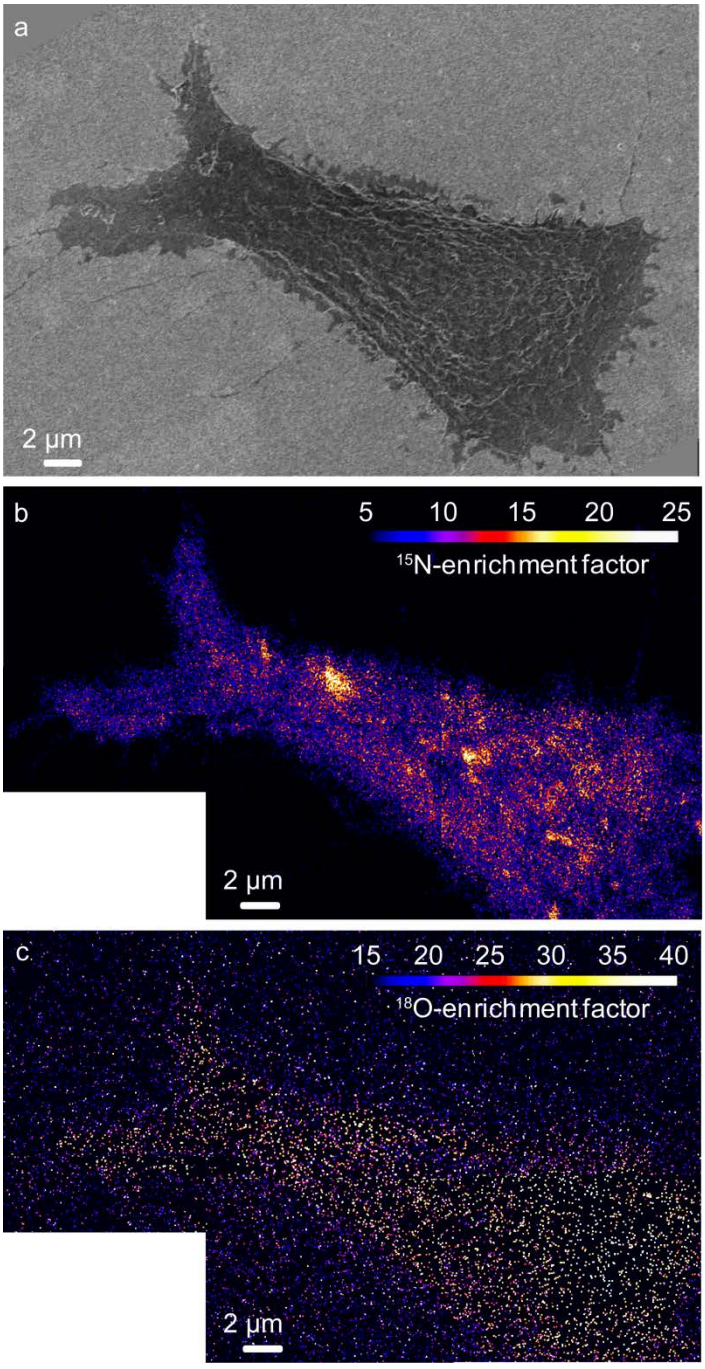

Figure 3. SEM and SIMS images of a metabolically labeled Clone 15 fibroblast cell that was treated with mβCD to reduce the cellular cholesterol by approximately 30%. (a) SEM image shows cell motphology. (b) The mosaic of 15 × 15 µm ^{15}N-enrichment images of the cell shows that mβCD treatment reduced the abundance of the ^{15}N-sphingolipid domains (orange and yellow regions) within the plasma membrane. (c) The mosaic of 15 × 15 µm ^{18}O-enrichment images of the cell shows the remaining ^{18}O-cholesterol is evenly distributed within the plasma membrane. Statistical tests confirmed the cholesterol abundance in the ^{15}N-sphingolipid domains did not differ from that in the non-domain regions of the plasma membrane (Kolmogorov-Smirnov test, p = 0.90).

References

1. F. R. Maxfield, A. K. Menon, Intracellular sterol transport and distribution. *Curr. Opin. Cell Biol.* **18**, 379 (2006).
2. M. Leslie, Do Lipid Rafts Exist? *Science* **334**, 1046 (November 25, 2011, 2011).
3. D. Lingwood, K. Simons, Lipid Rafts as an Organizing Principle. *Science* **327**, 46 (2010).
4. C. Eggeling *et al.*, Direct observation of the nanoscale dynamics of membrane lipids in a living cell. *Nature* **457**, 1159 (2009).
5. G. McMahon, B. J. Glassner, C. P. Lechene, Quantitative imaging of cells with multi-isotope imaging mass spectrometry (MIMS)--Nanoautography with stable isotope tracers. *Appl. Surf. Sci.* **252**, 6895 (2006).
6. C. R. Anderton, P. K. Weber, K. Lou, I. D. Hutcheon, M. L. Kraft, Correlated AFM and NanoSIMS imaging to probe cholesterol-induced changes in phase behavior and non-ideal mixing in ternary lipid membranes. *Biochim. Biophys. Acta* **1808**, 307 (2011).
7. M. L. Kraft, P. K. Weber, M. L. Longo, I. D. Hutcheon, S. G. Boxer, Phase Separation of Lipid Membranes Analyzed with High-Resolution Secondary Ion Mass Spectrometry. *Science* **313**, 1948 (September 29, 2006, 2006).
8. M. L. Steinhauser *et al.*, Multi-isotope imaging mass spectrometry quantifies stem cell division and metabolism. *Nature* **481**, 516 (2012).
9. H. A. Klitzing, P. K. Weber, M. L. Kraft, in *Methods in Molecular Biology: Nanoimaging Methods and Protocols* A. A. Sousa, M. J. Kruhlak, Eds. (Humana Press, Totowa, New Jersey, 2013), vol. 950, pp. 483-501.
10. R. L. Wilson *et al.*, Fluorinated Colloidal Gold Immunolabels for Imaging Select Proteins in Parallel with Lipids Using High-Resolution Secondary Ion Mass Spectrometry. *Bioconjugate Chem.* **23**, 450 (2012/02/15, 2012).
11. J. F. Frisz *et al.*, Direct chemical evidence for sphingolipid domains in the plasma membranes of fibroblasts. *Proc. Nat. Acad. Sci. U.S.A.*, 10.1073/pnas.1216585110 (January 28, 2013, 2013).
12. K. Simons, E. Ikonen, Functional rafts in cell membranes. *Nature* **387**, 569 (1997).
13. L. Bezrukov, P. S. Blank, I. V. Polozov, J. Zimmerberg, An adhesion-based method for plasma membrane isolation: Evaluating cholesterol extraction from cells and membranes. *Anal. Biochem.* **394**, 171 (2009).
14. S. L. Veatch, S. L. Keller, Miscibility phase diagrams of giant vesicles containing sphingomyelin. *Phys. Rev. Lett.* **94**, 148101(4) (2005).
15. K. Simons, M. J. Gerl, Revitalizing membrane rafts: new tools and insights. *Nat. Rev. Mol. Cell. Biol.* **11**, 688 (2010).
16. R. Zidovetzki, I. Levitan, Use of cyclodextrins to manipulate plasma membrane cholesterol content: Evidence, misconceptions, and control strategies. *Biochim. Biophys. Acta* **1768**, 1311 (2007).
17. L. Norman *et al.*, Modification of Cellular Cholesterol Content Affects Traction Force, Adhesion and Cell Spreading. *Cell. Mol. Bioeng.* **3**, 151 (2010).
18. M. Takahashi *et al.*, Cholesterol Controls Lipid Endocytosis through Rab11. *Mol. Biol. Cell* **18**, 2667 (May 2, 2007, 2007).
19. M. Reverter *et al.*, Cholesterol transport from late endosomes to the Golgi regulates t-SNARE trafficking, assembly, and function. *Mol. Biol. Cell* **22**, 4108 (November 1, 2011, 2011).

20. D. Goswami *et al.*, Nanoclusters of GPI-Anchored Proteins Are Formed by Cortical Actin-Driven Activity. *Cell* **135**, 1085 (2008).
21. K. Gowrishankar *et al.*, Active Remodeling of Cortical Actin Regulates Spatiotemporal Organization of Cell Surface Molecules. *Cell* **149**, 1353 (2012).